DOI: 10.1534/genetics.109.108878

Epithelial Polarity: Interactions Between Junctions and Apical–Basal Machinery

Nicole A. Kaplan, Xiaoping Liu and Nicholas S. Tolwinski[1]

Program in Developmental Biology, Sloan–Kettering Institute, Memorial Sloan–Kettering Cancer Center, New York, New York 10021

Manuscript received August 21, 2009
Accepted for publication September 1, 2009

ABSTRACT

Epithelial polarity is established and maintained by competition between determinants that define the apical and basolateral domains. Cell–cell adhesion complexes, or adherens junctions, form at the interface of these regions. Mutations in adhesion components as well as apical determinants normally lead to an expansion of the basolateral domain. Here we investigate the genetic relationship between the polarity determinants and adhesion and show that the levels of the adhesion protein Armadillo affect competition. We find that in *arm* mutants, even a modest reduction in the basolateral component *lgl* leads to a full apical domain expansion or *lgl* phenotype. By using an allelic series of Armadillo mutations, we show that there is a threshold at which basolateral expansion can be reversed. Further, in embryos lacking the Wingless signaling component *zw3*, the same full apical expansion occurs again with only a reduction in *lgl*. We propose a model where *zw3* regulates protein levels of apical and adhesion components and suggest that a reciprocal interaction between junctions and polarity modules functions to maintain stable apical and basolateral domains.

A major reason that epithelial cells require apical–basal polarity is to differentiate between the interior of the organism and the external environment. To accomplish this, epithelial cells generate molecularly distinct domains along their plasma membranes: an apical domain that is exposed to the outside, a basolateral domain that contacts the interior, and, in between, an adhesion complex that holds the cell sheet together. In Drosophila embryos, at least three polarity complexes are used to establish and maintain this subcellular organization commonly known as apical–basal cell polarity. On the apical side, the Crumbs (Crb) and Stardust (Std, Pals) proteins form one complex (Jurgens *et al.* 1984; Tepass *et al.* 1990; Tepass and Knust 1993; Wodarz *et al.* 1995; Muller and Wieschaus 1996). The second one is composed of Bazooka (Baz, Par-3), Par-6, and atypical protein kinase C (aPKC) (Wieschaus *et al.* 1984; Muller and Wieschaus 1996; Wodarz *et al.* 2000; Hutterer *et al.* 2004). On the opposite or basolateral side of the cell, Lethal giant larvae (Lgl), Discs large (Dlg), and Scribble (Scrib) determine the basolateral domain of the plasma membrane (Gateff and Schneiderman 1974; Mechler *et al.* 1985; Woods and Bryant 1989; Bilder and Perrimon 2000). In between the complexes lie the adherens junctions (AJ) composed of E-cadherin, Armadillo (Arm, β-catenin), and α-catenin (Oda *et al.* 1993, 1994; Peifer *et al.* 1993; Tepass *et al.* 1996).

In Drosophila embryos, mutations that affect apical components often lead to the *crumbs* phenotype, where ectodermal cells lose integrity and many die through apoptosis. The surviving cells secrete cuticle in a discontinuous fashion, leaving pieces apparently floating within the eggshell (Tepass *et al.* 1990; Tanentzapf and Tepass 2003). This phenotype is also seen in embryos deficient for AJ proteins (Oda *et al.* 1993; Cox *et al.* 1996; Magie *et al.* 2002). On the other hand, mutations that affect the basolateral genes display a very different phenotype. Zygotic only (Z) mutants for *scrib*, *lgl*, and *dlg* have a significant maternal mRNA contribution that allows normal embryonic development to proceed. Phenotypes are observed only in larvae, which die with significantly overgrown imaginal discs (Gateff 1978; Bilder and Perrimon 2000). Removal of the maternal mRNA complement, as well as the zygotic contribution (M/Z) through the induction of germline clones, leads to a poorly differentiated and convoluted cuticle with a bubbly appearance (Figure 1) (Bilder *et al.* 2003; Tanentzapf and Tepass 2003).

These studies led to a comprehensive competition model where apical and basal components opposed each other (Figure 1, schema); however, a strangely neglected topic was the interaction of junctions and the apical and basal determinants. Therefore, we used a genetic approach to investigate the interaction of apical–basal polarity proteins and adherens junctions.

[1]*Corresponding author:* Sloan–Kettering Institute, Memorial Sloan–Kettering Cancer Center, 1275 York Ave., Box 423, New York, NY 10021. E-mail: tolwinsn@mskcc.org

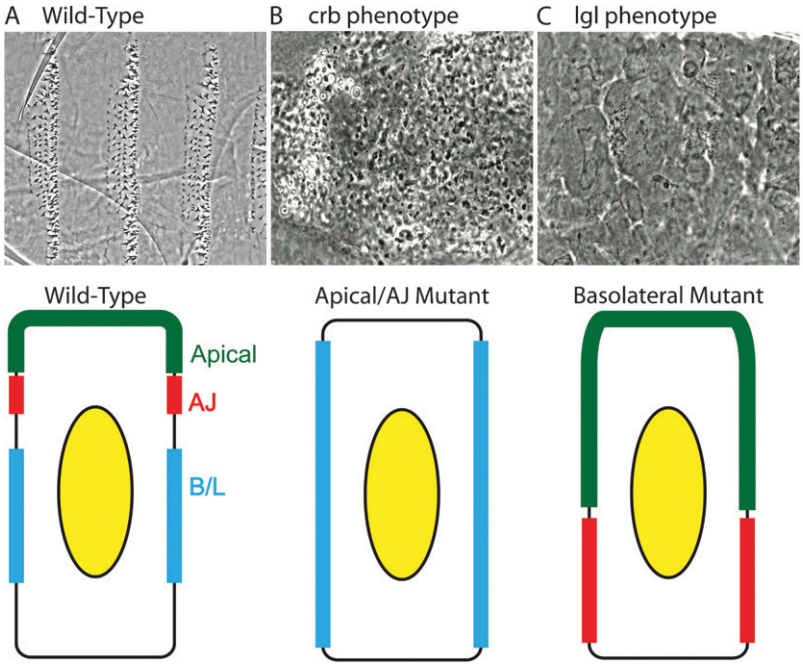

FIGURE 1.—Schema and cuticles representing wild-type *vs.* the opposing phenotypes of apical and basolateral expansion. (A) A wild-type cuticle shows rows of denticles separated by naked regions in a highly organized or patterned fashion. The apical determinants localize to the apical surface of cells, establishing the apical domain (green), the basolateral determinants localize to the basolateral surface of cells, establishing the basolateral domain (blue), and the adherens junctions (red) form at the interface between these two opposing regions. (B) The *crumbs* phenotype is observed when an apical determinant is mutated, causing an expansion of the basolateral domain. (C) The *lgl* phenotype, or bubble phenotype, is observed when a basolateral determinant is mutated, causing an expansion of the apical domain.

MATERIALS AND METHODS

Crosses and expression of UAS constructs: Maternally mutant eggs were generated by the dominant female sterile technique (CHOU and PERRIMON 1992). Oregon R was used as the wild-type strain. Please see FlyBase for details on mutants used (http://www.flybase.bio.indiana.edu). All mutants used were amorphs except for the *arm* mutants that were hypomorphs. The following crosses were conducted:

arm^{O43A01} FRT101/*OvoD1* FRT101 (chromosome 1) females
arm^{XM19} FRT101/*OvoD1* FRT101 females
arm^{F1a} FRT101/*OvoD1* FRT101 females
$zw3^{M11-1}$ FRT101/*OvoD1* FRT101 females
arm^{O43A01} FRT101/*OvoD1* FRT101; lgl^{4}/+ females × lgl^{4}/CyO males
arm^{XM19} FRT101/*OvoD1* FRT101; lgl^{4}/+ females × lgl^{4}/CyO males
arm^{F1a} FRT101/*OvoD1* FRT101; lgl^{4}/+ females × lgl^{4}/CyO males
$zw3^{M11-1}$ FRT101/*OvoD1* FRT101; lgl^{4}/+ females × lgl^{4}/CyO males
arm^{XM19} $zw3^{M11-1}$ FRT101/*OvoD1* FRT101; lgl^{4}/+ females × lgl^{4}/CyO males
arm^{F1a} $zw3^{M11-1}$ FRT101/*OvoD1* FRT101; lgl^{4}/+ females × lgl^{4}/CyO males
arm^{O43A01} FRT101/*OvoD1* FRT101; $aPKC^{K06403}$/+ females × $aPKC^{K06403}$/CyO males
arm^{XM19} FRT101/*OvoD1* FRT101; $aPKC^{K06403}$/+ females × $aPKC^{K06403}$/CyO males
arm^{F1a} FRT101/*OvoD1* FRT101; $aPKC^{K06403}$/+ females × $aPKC^{K06403}$/CyO males
$zw3^{M11-1}$ FRT101/*OvoD1* FRT101; $aPKC^{K06403}$/+ females × $aPKC^{K06403}$/CyO males
arm^{XM19} $zw3^{M11-1}$ FRT101/*OvoD1* FRT101; $aPKC^{K06403}$/+ females × $aPKC^{K06403}$/CyO males
arm^{F1a} $zw3^{M11-1}$ FRT101/*OvoD1* FRT101; $aPKC^{K06403}$/+ females × $aPKC^{K06403}$/CyO males
arm^{O43A01}, dlg^{G0276} FRT19A/*OvoD2* FRT19A females
arm^{O43A01} FRT101/*OvoD1* FRT101 females; *arm-GAL4*/+ × w; *UAS-crumbs* males
Frt40A, lgl^{4}/Frt40A *OvoD1* females × lgl^{4}/CyO males
FrtG13, $aPKC^{K06403}$/FrtG13 *OvoD1* females × $aPKC^{K06403}$/CyO males.

Antibodies and immunofluorescence: Embryos were fixed with heat–methanol treatment (MULLER and WIESCHAUS 1996). The antibodies used were anti-α-catenin [ratAb DCAT, Developmental Studies Hybridoma Bank (DSHB), developed under the auspices of the National Institute of Child Health and Human Development and maintained by The University of Iowa, Department of Biological Sciences, Iowa City, IA], anti-Armadillo (mAb N2 7A1, DSHB), anti-β-tubulin (E7, DSHB), anti-E-Cadherin (ratAb ECAD2, DSHB), and rabbit and goat anti-aPKCζ (Santa Cruz Biotechnology). Cuticle preparations, staining, detection, and image processing were as described in COLOSIMO and TOLWINSKI (2006).

Western blotting: Embryos were lysed in extract buffer (50 mM Tris, pH 7.5, 150 mM NaCl, 1% NP-40, 1 mM EDTA, 10% glycerol; Complete Mini Protease, Sigma, St. Louis) or RIPA lysis buffer (Santa Cruz Biotechnology). The extracts were separated by 7.5% SDS–PAGE and blotted as described in PEIFER *et al.* (1994). Extracts were normalized using the BCA assay (Novagen). Overnight embryo collections were used to make extracts for Western blots.

RESULTS AND DISCUSSION

Loss of *arm* enhances *lgl* phenotypes: In Drosophila embryos, mutations in basolateral components led to an expansion of the apical region or the *lgl* phenotype, whereas mutations in apical components led to a basolateral expansion or the *crumbs* phenotype (Figure 1). These opposite phenotypes provided a simple assay for us to investigate the genetic interactions between apical–basal polarity components and adherens junctions. Specifically, we used a series of double mutants composed of an allelic series of mutations affecting the AJ component *arm* and strong loss-of-function mutations in apical and basolateral components. For this experiment, we used three *arm* mutants: arm^{O43A01}, which

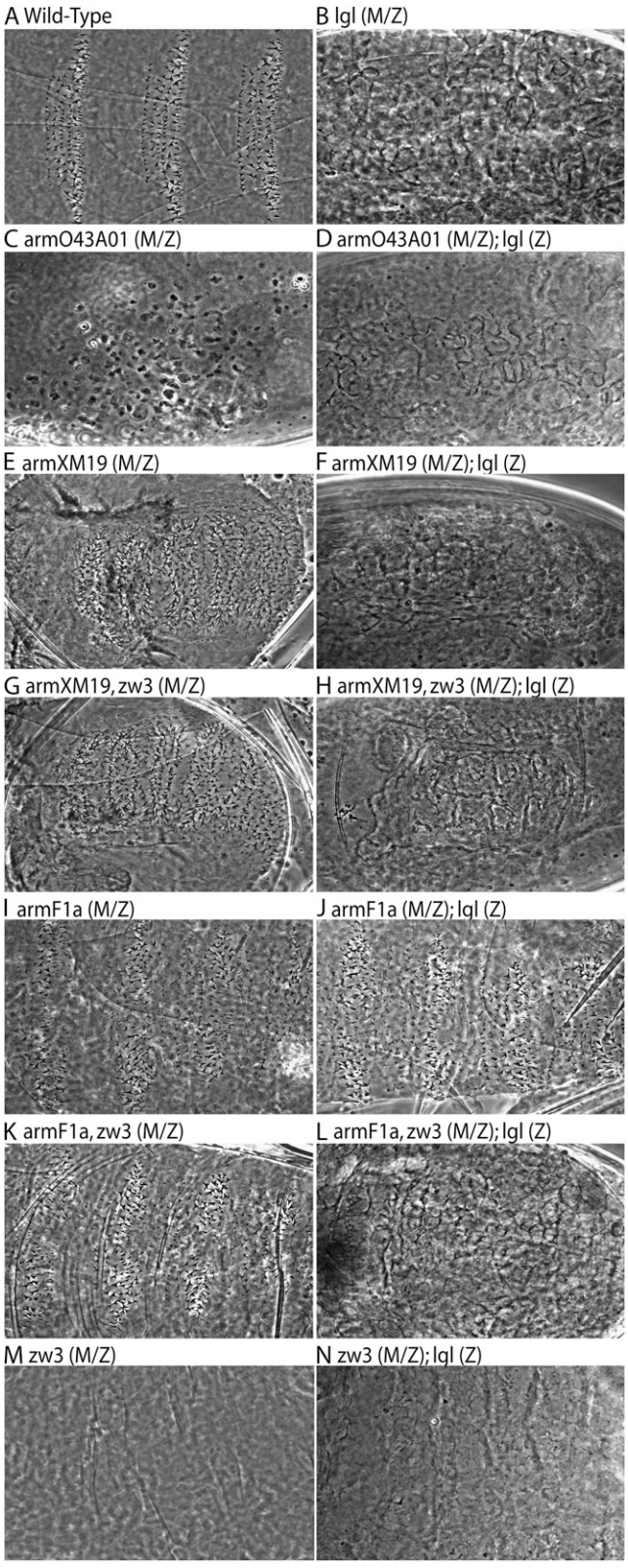

Figure 2.—Zygotic loss of *lgl* is epistatic to *arm* phenotypes. (A) Wild type: cuticle displays highly organized rows of denticles. (B) *lgl* (M/Z): bubble phenotype. A convoluted cuticle forms in these embryos. (C) arm^{O43A01} (M/Z): crumbs phenotype. Cuticle fails to form, leaving pieces randomly dispersed in the embryo. (D) arm^{O43A01} (M/Z); *lgl* (Z): a rescue of the crumbs phenotype. Some cuticle forms, which appears similar to the *lgl* phenotype. (E) arm^{XM19} (M/Z): loss of naked cuticle regions, strong *wg* phenotype. (F) arm^{XM19} (M/Z); *lgl* (Z): with a zygotic only loss of *lgl*, cuticle is similar to the *lgl* phenotype. (G) arm^{XM19} (M/Z), *zw3* (M/Z): cuticle resembles E above; the introduction of the *zw3* mutation seems to have little to no effect. (H) arm^{XM19} (M/Z), *zw3* (M/Z); *lgl* (Z): with a zygotic only loss of *lgl*, cuticle is similar to the *lgl* phenotype. (I) arm^{F1a} (M/Z): loss of naked cuticle regions, weak *wg* phenotype. (J) arm^{F1a} (M/Z); *lgl* (Z): cuticle resembles I above; the *lgl* phenotype is not observed. (K) arm^{F1a} (M/Z), *zw3* (M/Z): cuticle resembles I above; the introduction of the *zw3* mutation seems to have little to no effect. (L) arm^{F1a} (M/Z), *zw3* (M/Z); *lgl* (Z): with the introduction of *lgl* (Z), cuticle appears similar to the *lgl* phenotype. (M) *zw3* (M/Z): naked cuticle. No cells secrete denticles, as *wg* signaling is hyperactivated. (N) *zw3* (M/Z); *lgl* (Z): with zygotic only loss of *lgl*, cuticle is similar to the *lgl* phenotype.

deletes the final three repeats and the entire COOH terminus of the protein leading to severe adhesion defects; arm^{XM19}, a mutation that deletes only the COOH terminus and blocks Wingless signaling while leaving adhesion relatively intact; and arm^{F1a}, a point mutation that leaves embryos completely intact with only a weak effect on patterning (Peifer and Wieschaus 1990; Cox *et al.* 1999; Tolwinski and Wieschaus 2004a). This series of hypomorphic alleles allowed for precise modulation of *arm* activity. The protein levels were affected, in that the two truncation alleles were expressed at low levels due to nonsense-mediated decay, whereas the point mutant was expressed at wild-type levels since it was not affected by nonsense-mediated RNA decay (Wagner and Lykke-Andersen 2002).

To investigate the effect of basolateral components on adhesion, we made *arm* and *lgl* double mutants. In these experiments, *arm* mutants were germline clones or maternally and zygotically mutant (M/Z), whereas *lgl* was only zygotically mutant (Z). Interestingly, we found that in the strongest arm^{O43A01} mutant where adherens junctions were lost and epithelia degenerated into a *crumbs*-like phenotype, the additional loss of *lgl* led to the bubbly cuticle completely suppressing the *crumbs* phenotype (Figure 2, C and D, Table 1). Patterning of the cuticle was still disrupted, as *lgl* does not function in the canonical Wg pathway. This result suggested that though loss of adherens junctions normally led to an expansion of the basolateral domain, the additional loss of the basolateral determinant *lgl* restored a full apical expansion phenotype or the *crumbs* cuticle (Figure 4C, schema).

Next, we looked at the intermediate arm^{XM19} mutant and saw a similar effect where zygotic loss of *lgl* led to the bubbly cuticle phenotype (Figure 2, E and F, Table 1). This result was surprising as this mutant showed an intact epithelium, suggesting that adherens junctions are functional. However, Arm protein levels in this mutant are much lower (Peifer and Wieschaus 1990), which perhaps led to a weakening of junctions and an apical expansion phenotype when *lgl* was mutated additionally.

In contrast to these findings, when we looked at the weakest and most strongly expressed arm^{F1a} mutant in

TABLE 1

Genetic interactions between apical or basal components and *arm*

Genetic combination	Embryonic cuticle effect	Predicted %
arm^{O43A01} (M/Z)	*crumbs*	50
arm^{XM19} (M/Z)	Patterning (*wg*)	50
arm^{F1a} (M/Z)	Patterning (*wg*)	50
$zw3^{M11-1}$ (M/Z)	Patterning (Naked)	50
arm^{O43A01} (M/Z); $l(2)gl^{4}$ (Z)	*lgl*: 20/158	12.5
arm^{XM19} (M/Z); $l(2)gl^{4}$ (Z)	*lgl*: 26/164	12.5
arm^{F1a} (M/Z); $l(2)gl^{4}$ (Z)	Patterning (*wg*): 52/101	50
$zw3^{M11-1}$ (M/Z); $l(2)gl^{4}$ (Z)	*lgl*: 15/110, 12.5% expected	12.5
arm^{XM19}, $zw3^{M11-1}$ (M/Z); $l(2)gl^{4}$ (Z)	*lgl*: 23/160, 12.5% expected	12.5
arm^{F1a}, $zw3^{M11-1}$ (M/Z); $l(2)gl^{4}$ (Z)	*lgl*: 51/103, 12.5% expected	12.5
arm^{O43A01} (M/Z); $apkc^{K06403}$ (Z)	*crumbs*: 31/63	50
arm^{XM19} (M/Z); $apkc^{K06403}$ (Z)	Patterning (*wg*): 43/98	50
arm^{F1a} (M/Z); $apkc^{K06403}$ (Z)	Patterning (*wg*): 62/113	50
$zw3^{M11-1}$ (M/Z); $apkc^{K06403}$ (Z)	Patterning (Naked): 74/138	50
arm^{XM19}, $zw3^{M11-1}$ (M/Z); $apkc^{K06403}$ (Z)	Patterning (*wg*): 33/61	50
arm^{F1a}, $zw3^{M11-1}$ (M/Z); $apkc^{K06403}$ (Z)	Patterning (*wg*): 48/102	50
arm^{O43A01}, dlg^{G0276} (M/Z)	*lgl*: 107/204	50
arm^{O43A01}(M/Z); *arm*-GAL4/UAS-*crumbs*	*lgl*: 60/123	50
$l(2)gl^{4}$ (Z)	Wild type: Hatch	~100
$apkc^{K06403}$ (Z)	Wild type: Hatch	~100
$l(2)gl^{4}$ (M/Z)	*Lgl*	50
$apkc^{K06403}$ (M/Z)	*Crumbs*	50

Column 1 shows the genetic combination assayed for genotype. Column 2 presents the phenotype that we observed for the mutant combinations as well as a quantification of the mutant embryos found (specific mutant phenotype/total). Column 3 presents the expected ratio for interaction if it occurred or for noninteraction if we did not find one. Specifically, for double or triple mutants 12.5% is the predicted ratio for a fully penetrant phenotype or if *lgl* is completely epistatic to *arm*. For noninteraction, we expect 50% of the embryos to show the *arm* or X chromosome-linked phenotype. Similarly, for *aPKC* mutants that do not interact, we expect 50% of the embryos to show the *arm* or X chromosome-linked phenotype. Both *dlg* and *arm* are on the X chromosome so the double mutant phenotype is expected in half the embryos if fully penetrant, and half the embryos overexpress UAS-Crb so 50% should show the *crb* phenotype. For a full list of genotypes used in the crosses please see MATERIALS AND METHODS. The crosses were scored by cuticle prep and assigned into categories on the basis of apparent phenotype and expected Mendelian genetic ratios. Most X chromosome mutants additionally carried the *y* mutation, which is visible under brightfield illumination, aiding identification of hemizygous embryos. The numbers in column 2 are from a representative experiment of several conducted.

combination with *lgl*, no effect was observed (Figure 2, I and J, Table 1). In this mutant only an effect on patterning was observed regardless of whether *lgl* was mutant or not. This result suggested that similarly to the wild-type situation, arm^{F1a} mutants maintained junctions at a sufficient level to prevent the zygotic loss of *lgl* from causing a full apical expansion phenotype. Therefore, in contrast to *arm* mutants where protein levels are low, arm^{F1a} can maintain apical–basal domain stability. Taken together, these results showed that lowering the levels of Arm protein, and thereby affecting AJs, led to a strong enhancement of the *lgl* phenotype. This finding was surprising, because *lgl* zygotic mutants should retain a significant maternal mRNA contribution that normally allows them to complete embryogenesis, yet we observed a full apical expansion phenotype in zygotic mutants alone.

***lgl* and *arm* double mutants show apical expansion:** To analyze the *lgl* phenotype further, we looked at the expression of apical and AJ markers in these mutants. Wild-type embryos have epithelia that maintain separate domains in the apical–basal direction. To demonstrate this we used the markers aPKC for apical and Arm for AJs (Figure 3, A and A′). In arm^{O43A01} mutants, epithelial cells lost adhesion as AJs were unstable and were lost from many cells (Figure 3B). Additionally, the apical domain disappeared as aPKC staining was greatly reduced (Figure 3B′). When these embryos carried an additional zygotic mutation in *lgl*, the phenotype was reversed, and Arm and aPKC expanded to the entire plasma membrane (Figure 3, D and D′). This phenotype was very similar to that observed for *lgl* (M/Z) mutants (Figure 3, C and C′); however, these embryos lacked both the maternal and the zygotic contributions

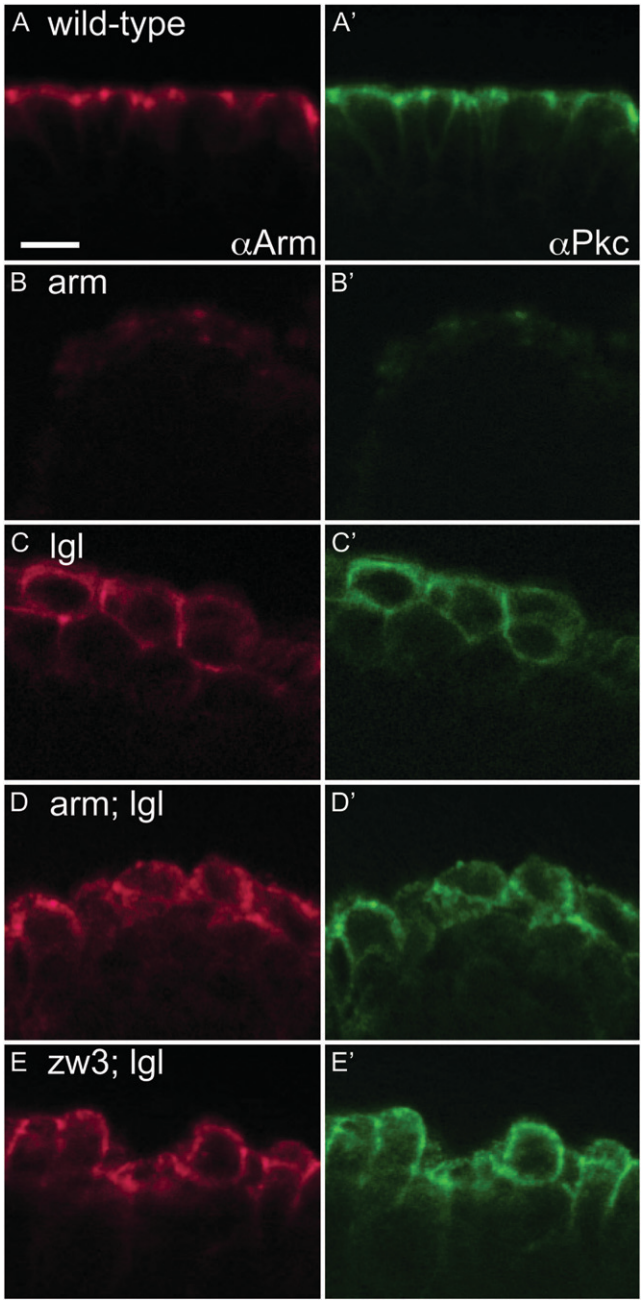

Figure 3.—A reduction in basolateral determinant *lgl* leads to a full apical expansion phenotype, resembling the *lgl* (M/Z) phenotype, shown by the localization of the apical marker (aPKC) and the junctional marker (Arm), in cross-sections of mutant embryos. (A and A′) Wild-type (A) Arm localizes to the adherens junctions along the apical membrane. (A′) aPKC localizes slightly more apically. (B and B′) arm^{043A01} (M/Z) cells lose adherens junctions; Arm is absent from the apical membrane. (B′) Loss of apical component: aPKC staining is significantly reduced at the apical membrane. (C) *lgl* (M/Z), (D) arm^{043A01}; *lgl*, and (E) *zw3*; *lgl*: D and E resemble C, the *lgl* (M/Z) phenotype. (C–E) Arm staining now encircles the entire membrane, showing a full apical expansion down the basolateral surfaces. (C′–E′) The apical marker aPKC is also expanded along the basolateral membrane in these mutants. Bar, 5 μm.

of *lgl* mRNA, whereas the arm^{O43A01}, *lgl* double had the maternal contribution of *lgl* mRNA. Overall, our data support the genetic model of apical *vs.* basolateral competition shown genetically and cell biologically (Bilder *et al.* 2003; Tanentzapf and Tepass 2003). Our cell biological results were observed at mid- to late embryonic stages since at early stages domain expansions are not obvious (Blankenship *et al.* 2007), and at late stages there is some recovery (Laprise *et al.* 2009).

Zw3 kinase regulates apical–basal domain stability: Wingless (Wg/Wnt) pathways can affect the polarity of cells both through effects on apical–basal components and junctions (Etienne-Manneville and Hall 2003; Etienne-Manneville *et al.* 2005; Colosimo and Tolwinski 2006; Schlessinger *et al.* 2007; Yamanaka and Nishida 2007; Schlessinger *et al.* 2009). We have previously shown that the kinase Zw3 (also known as glycogen synthase kinase 3β) can function to regulate the levels of aPKC protein. In the absence of *zw3*, aPKC protein levels increased, and led to the apical expansion or *lgl* phenotype (Colosimo *et al.* 2009). We therefore asked whether the additional loss of *zw3* could enhance the phenotypes we observed for *arm* and *lgl* alone. We began by investigating the genetic interaction of *zw3* and *lgl*. Mutations in *zw3* led to the ectopic activation of Wg signaling in all cells of the embryonic epidermis and a cuticle characterized by a complete loss of denticles [Figure 2M (Hatini and Dinardo 2001)]. In the double mutant, *zw3* (M/Z); *lgl* (Z), we observed *lgl*-like cuticles (Figure 2N). Closer, cell biological investigation revealed that the epithelia appeared similar to the *lgl* (M/Z) mutant alone, with the full apical expansion phenotype for both junctions and aPKC (compare Figure 3C and 3C′ to 3E and 3E′). Therefore, loss of *zw3* kinase can lead to an apical expansion phenotype with only zygotic loss of *lgl*, likely through an increase in aPKC protein levels (see model in Figure 4B).

Zw3 kinase regulates apical–basal domain stability independently of canonical Wg signal: As the loss of *zw3* leads to ectopic canonical Wg signaling activation (Tolwinski and Wieschaus 2004b), we investigated the effect of Zw3 on polarity in mutant backgrounds where the downstream response was abrogated with an additional mutation in *arm* that should block the transcriptional response (Tolwinski *et al.* 2003). To accomplish this, we made triple mutants of *arm*, *lgl*, and *zw3*. As we have shown above, both arm^{XM19} (M/Z); *lgl* (Z) and *zw3* (M/Z); *lgl* (Z) cuticles take on the apical expansion or *lgl* phenotype. We therefore anticipated that arm^{XM19}, *zw3* (M/Z); *lgl* (Z) triple mutants would also show the *lgl* phenotype. Indeed, these embryos were very similar in appearance to arm^{XM19} (M/Z), *lgl* (Z) alone (compare Figure 2E and 2F to 2G and 2H).

In contrast to the arm^{XM19} results, the arm^{F1a} mutant was unaffected by loss of *lgl* (Figure 2J), but surprisingly we observed that the combination of arm^{F1a}, *zw3* (M/Z), *lgl* (Z) triple mutants gave the *lgl* phenotype (Figure

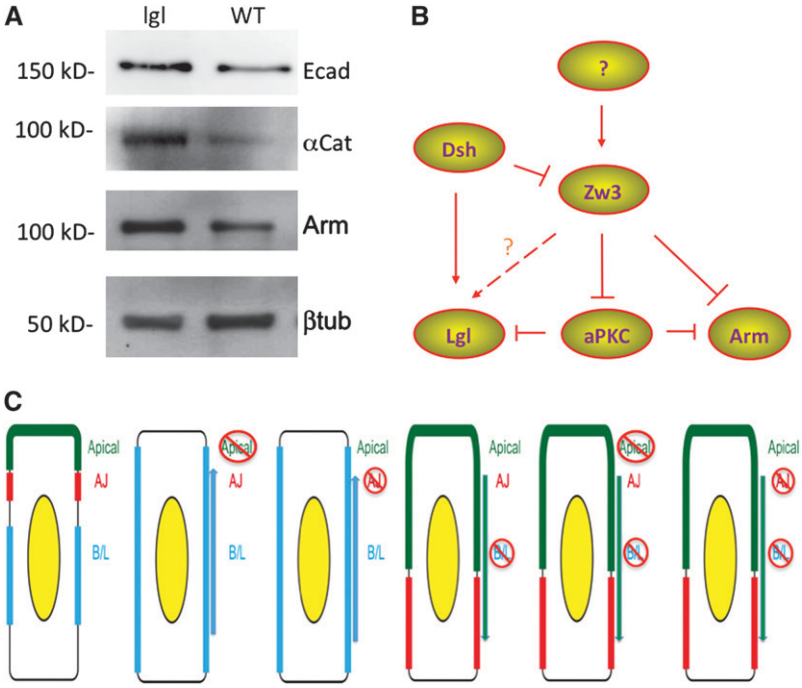

Figure 4.—Armadillo, E-cadherin, and α-catenin protein levels are increased significantly in *lgl* mutants, suggesting that the loss of *lgl* stabilizes adherens junctions. (A) Western blot comparing Armadillo, E-cadherin, and α-catenin protein levels in wild-type *vs. lgl* (M/Z) mutants, with β-tubulin used as a loading control. (B) Overall model of polarity regulation by Zw3 where it regulated the protein levels of both Arm and aPKC. Zw3's effect on Lgl is most likely indirect through its regulation of aPKC, but there may be a direct effect as well. One known upstream component is Dsh, which has a direct effect on both Zw3 and Lgl, but what signals are upstream of both of these molecules remains to be discovered. (C) Schematic representation of the genetic results from single and double mutants in the apical–basal and AJ machinery translated into predicted cell biological effects.

2L). A possible explanation for this result is that the increase in aPKC levels in *zw3* mutants could expand the apical domain sufficiently to tip the apical–basal polarity balance toward the *lgl* phenotype even in the relatively intact arm^{F1a} mutants. Further, by using the double-mutant arm^{F1a}, *zw3* (M/Z), we blocked the canonical Wg signaling pathway at the transcriptional step or downstream of Zw3, therefore suggesting that the function of Zw3 in this process is not through transcription and actually more similar to noncanonical Wnt signaling pathways (Simons and Mlodzik 2008; Schlessinger *et al.* 2009).

Arm protein levels are increased in *lgl* mutants: We have previously shown that in *zw3* mutants there is a recognizable effect on apical–basal polarity. This occurs because *zw3* regulates the levels of *aPKC*, and excess aPKC tends to expand the apical domain (Colosimo *et al.* 2009). Additionally, we have shown that aPKC expands the apical domain by stabilizing the levels of Arm protein at the membrane (Colosimo *et al.* 2009). In *zw3* (M/Z), *lgl* (Z) double mutants a similar apical expansion occurs, and since hyperactivation of aPKC should in principle be identical to loss of *lgl* (Betschinger *et al.* 2003), we looked at Arm protein levels in *lgl* mutants. We compared the total levels of Arm protein in *lgl* mutants to those in wild-type embryos. Arm protein levels were significantly increased in *lgl* mutants as compared to the wild-type control (Figure 4A). Indeed, the protein levels of core AJ components α-catenin and E-cadherin were also increased (Figure 4A). These results suggest that loss of *lgl*, in a manner similar to the gain-of-function aPKC, results in stabilization of junctions through an increase in AJ protein levels. Further, this increase likely occurs in the membrane fraction and not in the canonical Wnt signaling pool, as patterning is not affected in either *lgl* mutants or aPKC overexpressing embryos [Figure 1C (Gottardi and Gumbiner 2004; Colosimo *et al.* 2009)].

We further tested the *arm* alleles or *arm, zw3* (M/Z) double mutants in combination with an *aPKC* (Z) allele, but did not observe an effect of apical–basal polarity (Table 1). The expected result would have been a tilt toward the *crumbs* phenotype, but this was not observed. One explanation is that the maternal contribution of aPKC is sufficient to overcome the zygotic mutation. However, another possibility is that the effect we observe is specific to basolateral components, where one of the functions of the AJ is to prevent the expansion of apical components into the basolateral domain. This model would be consistent with the currently understood mechanism of polarity, as aPKC can phosphorylate and dislodge Lgl from the membrane (Betschinger *et al.* 2003). Therefore, AJs may physically separate aPKC from Lgl, maintaining the basolateral domain (Figure 4C, model). Unfortunately, we were not able to further characterize this, because (M/Z) mutants of apical components such as *aPKC*, *par-6*, and arm^{O43A01}*par-6* double mutants have a very strong *crumbs* phenotype, making further dissection problematic (data not shown).

Previous work has shown that in *arm* mutants Dlg is mislocalized to the apical surface, suggesting a basolateral expansion (Harris and Peifer 2004). Further, loss of *baz* or *crb* leads to a loss of adherens junctions (Grawe *et al.* 1996; Klebes and Knust 2000; Harris and Peifer 2005; Harris and Tepass 2008), whereas loss of *lgl* leads to a lateral expansion of the zonula

adherens (Bilder *et al.* 2003; Tanentzapf and Tepass 2003). Adherens junctions form at the border of the apical and basolateral complexes. These two complexes are competing, and therefore mutating components of one lead to the other one winning and expanding into the former's domain. Loss of adherens junctions leads to a basolateral expansion similar to loss of apical components (Bilder *et al.* 2003; Tanentzapf and Tepass 2003; Blankenship *et al.* 2007). Consistent with this role, aPKC and Baz have been shown to regulate AJ formation (Harris and Peifer 2004, 2005; Colosimo *et al.* 2009). Our results suggest that a major function of AJs may be to keep the apical complex away from Lgl, as even a mild loss of a basolateral component can result in apical expansion.

Overall our experiments suggest that AJs behave genetically similarly to apical components. Namely, loss of adhesion leads to a basolateral expansion. However, they have a further function in preventing the apical domain from expanding when aPKC levels increase, and they prevent apical expansion when basolateral determinants are mildly affected. This finding offers the first genetic evidence that AJs behave as barriers between cellular domains. The regulation of these domains appears to be complex, as evidence points to Wnt signaling components playing a role in all three regions (Etienne-Manneville and Hall 2003; Etienne-Manneville *et al.* 2005; Colosimo and Tolwinski 2006; Schlessinger *et al.* 2007, 2009; Yamanaka and Nishida 2007). Zw3 can regulate the levels of aPKC and Arm proteins and Lgl is regulated by another Wnt component Disheveled that in turn inhibits Zw3 (Figure 4B). However, the function of Wnt signals in apical–basal polarity is poorly defined and will need to be the subject of further studies.

Finally, the kinase Zw3 (GSK3β) functions as a tumor suppressor by preventing the accumulation of the oncogenic protein Arm (β-catenin). Additionally, Lgl is a tumor suppressor protein that prevents overgrowth of epithelial cells (Hariharan and Bilder 2006). Our results link polarity and the oncogenic potential of the Wnt pathway, suggesting that Wnt pathway mutations lead to misregulation of cell polarity in addition to loss of proliferation control (Reya and Clevers 2005). One possible complication is that previous work showed that the loss of basolateral components leads to overgrowth, whereas loss of apical components or junctions leads to cell death (Kim *et al.* 2007; Humbert *et al.* 2008). Therefore Lgl must be pro-apoptotic and the maintenance of apical complexes and adhesion must be anti-apoptotic. This appears to be a contradiction, as loss of adhesion is associated with metastatic cancers, although further work will be required to address this question.

We thank Andreas Wodarz and Jurgen Knoblich for sharing reagents. This work was supported by the Frank A. Howard Fellows Program at the Sloan–Kettering Institute.

LITERATURE CITED

Betschinger, J., K. Mechtler and J. A. Knoblich, 2003 The Par complex directs asymmetric cell division by phosphorylating the cytoskeletal protein Lgl. Nature **422:** 326–330.

Bilder, D., and N. Perrimon, 2000 Localization of apical epithelial determinants by the basolateral PDZ protein Scribble. Nature **403:** 676–680.

Bilder, D., M. Schober and N. Perrimon, 2003 Integrated activity of PDZ protein complexes regulates epithelial polarity. Nat. Cell Biol. **5:** 53–58.

Blankenship, J. T., M. T. Fuller and J. A. Zallen, 2007 The Drosophila homolog of the Exo84 exocyst subunit promotes apical epithelial identity. J. Cell Sci. **120:** 3099–3110.

Chou, T. B., and N. Perrimon, 1992 Use of a yeast site-specific recombinase to produce female germline chimeras in Drosophila. Genetics **131:** 643–653.

Colosimo, P. F., and N. S. Tolwinski, 2006 Wnt, Hedgehog and junctional Armadillo/beta-catenin establish planar polarity in the Drosophila embryo. PLoS ONE **1:** e9.

Colosimo, P. F., X. Liu, N. A. Kaplan and N. S. Tolwinski, 2009 GSK3beta affects apical-basal polarity and cell-cell adhesion by regulating aPKC levels. Dev. Dyn. (in press).

Cox, R. T., C. Kirkpatrick and M. Peifer, 1996 Armadillo is required for adherens junction assembly, cell polarity, and morphogenesis during Drosophila embryogenesis. J. Cell Biol. **134:** 133–148.

Cox, R. T., L. M. Pai, C. Kirkpatrick, J. Stein and M. Peifer, 1999 Roles of the C terminus of Armadillo in Wingless signaling in Drosophila. Genetics **153:** 319–332.

Etienne-Manneville, S., and A. Hall, 2003 Cdc42 regulates GSK-3beta and adenomatous polyposis coli to control cell polarity. Nature **421:** 753–756.

Etienne-Manneville, S., J. B. Manneville, S. Nicholls, M. A. Ferenczi and A. Hall, 2005 Cdc42 and Par6-PKCzeta regulate the spatially localized association of Dlg1 and APC to control cell polarization. J. Cell Biol. **170:** 895–901.

Gateff, E., 1978 Malignant neoplasms of genetic origin in Drosophila melanogaster. Science **200:** 1448–1459.

Gateff, E., and H. A. Schneiderman, 1974 Developmental capacities of benign and malignant neoplasms of Drosophila. Roux's Arch. Dev. Biol. **176:** 23–65.

Gottardi, C. J., and B. M. Gumbiner, 2004 Distinct molecular forms of beta-catenin are targeted to adhesive or transcriptional complexes. J. Cell Biol. **167:** 339–349.

Grawe, F., A. Wodarz, B. Lee, E. Knust and H. Skaer, 1996 The Drosophila genes crumbs and stardust are involved in the biogenesis of adherens junctions. Development **122:** 951–959.

Hariharan, I. K., and D. Bilder, 2006 Regulation of imaginal disc growth by tumor-suppressor genes in Drosophila. Annu. Rev. Genet. **40:** 335–361.

Harris, K. P., and U. Tepass, 2008 Cdc42 and Par proteins stabilize dynamic adherens junctions in the Drosophila neuroectoderm through regulation of apical endocytosis. J. Cell Biol. **183:** 1129–1143.

Harris, T. J., and M. Peifer, 2004 Adherens junction-dependent and -independent steps in the establishment of epithelial cell polarity in Drosophila. J. Cell Biol. **167:** 135–147.

Harris, T. J., and M. Peifer, 2005 The positioning and segregation of apical cues during epithelial polarity establishment in Drosophila. J. Cell Biol. **170:** 813–823.

Hatini, V., and S. DiNardo, 2001 Divide and conquer: pattern formation in Drosophila embryonic epidermis. Trends Genet. **17:** 574–579.

Humbert, P. O., N. A. Grzeschik, A. M. Brumby, R. Galea, I. Elsum *et al.*, 2008 Control of tumourigenesis by the Scribble/Dlg/Lgl polarity module. Oncogene **27:** 6888–6907.

Hutterer, A., J. Betschinger, M. Petronczki and J. A. Knoblich, 2004 Sequential roles of Cdc42, Par-6, aPKC, and Lgl in the establishment of epithelial polarity during Drosophila embryogenesis. Dev. Cell **6:** 845–854.

Jurgens, G., E. Wieschaus, C. Nusslein-Volhard and H. Kluding, 1984 Mutations affecting the pattern of the larval cuticle in Drosophila melanogaster. II. Zygotic loci on the third chromosome. Roux's Arch. Dev. Biol. **193:** 283–295.

Kim, M., A. Datta, P. Brakeman, W. Yu and K. E. Mostov, 2007 Polarity proteins PAR6 and aPKC regulate cell death

through GSK-3beta in 3D epithelial morphogenesis. J. Cell Sci. **120:** 2309–2317.

Klebes, A., and E. Knust, 2000 A conserved motif in Crumbs is required for E-cadherin localisation and zonula adherens formation in Drosophila. Curr. Biol. **10:** 76–85.

Laprise, P., K. M. Lau, K. P. Harris, N. F. Silva-Gagliardi, S. M. Paul *et al.*, 2009 Yurt, Coracle, Neurexin IV and the Na(+),K(+)-ATPase form a novel group of epithelial polarity proteins. Nature **459:** 1141–1145.

Magie, C. R., D. Pinto-Santini and S. M. Parkhurst, 2002 Rho1 interacts with p120ctn and alpha-catenin, and regulates cadherin-based adherens junction components in Drosophila. Development **129:** 3771–3782.

Mechler, B. M., W. McGinnis and W. J. Gehring, 1985 Molecular cloning of lethal(2)giant larvae, a recessive oncogene of Drosophila melanogaster. EMBO J. **4:** 1551–1557.

Muller, H. A., and E. Wieschaus, 1996 armadillo, bazooka, and stardust are critical for early stages in formation of the zonula adherens and maintenance of the polarized blastoderm epithelium in Drosophila. J. Cell Biol. **134:** 149–163.

Oda, H., T. Uemura, K. Shiomi, A. Nagafuchi, S. Tsukita *et al.*, 1993 Identification of a Drosophila homologue of alpha-catenin and its association with the armadillo protein. J. Cell Biol. **121:** 1133–1140.

Oda, H., T. Uemura, Y. Harada, Y. Iwai and M. Takeichi, 1994 A Drosophila homolog of cadherin associated with armadillo and essential for embryonic cell-cell adhesion. Dev. Biol. **165:** 716–726.

Peifer, M., and E. Wieschaus, 1990 The segment polarity gene armadillo encodes a functionally modular protein that is the Drosophila homolog of human plakoglobin. Cell **63:** 1167–1176.

Peifer, M., S. Orsulic, D. Sweeton and E. Wieschaus, 1993 A role for the Drosophila segment polarity gene armadillo in cell adhesion and cytoskeletal integrity during oogenesis. Development **118:** 1191–1207.

Peifer, M., L. M. Pai and M. Casey, 1994 Phosphorylation of the Drosophila adherens junction protein Armadillo: roles for wingless signal and zeste-white 3 kinase. Dev. Biol. **166:** 543–556.

Reya, T., and H. Clevers, 2005 Wnt signalling in stem cells and cancer. Nature **434:** 843–850.

Schlessinger, K., E. J. McManus and A. Hall, 2007 Cdc42 and noncanonical Wnt signal transduction pathways cooperate to promote cell polarity. J. Cell Biol. **178:** 355–361.

Schlessinger, K., A. Hall and N. Tolwinski, 2009 Wnt signaling pathways meet Rho GTPases. Genes Dev. **23:** 265–277.

Simons, M., and M. Mlodzik, 2008 Planar cell polarity signaling: from fly development to human disease. Annu. Rev. Genet. **42:** 517–540.

Tanentzapf, G., and U. Tepass, 2003 Interactions between the crumbs, lethal giant larvae and bazooka pathways in epithelial polarization. Nat. Cell Biol. **5:** 46–52.

Tepass, U., and E. Knust, 1993 Crumbs and stardust act in a genetic pathway that controls the organization of epithelia in Drosophila melanogaster. Dev. Biol. **159:** 311–326.

Tepass, U., C. Theres and E. Knust, 1990 crumbs encodes an EGF-like protein expressed on apical membranes of Drosophila epithelial cells and required for organization of epithelia. Cell **61:** 787–799.

Tepass, U., E. Gruszynski-DeFeo, T. A. Haag, L. Omatyar, T. Torok *et al.*, 1996 shotgun encodes Drosophila E-cadherin and is preferentially required during cell rearrangement in the neurectoderm and other morphogenetically active epithelia. Genes Dev. **10:** 672–685.

Tolwinski, N. S., and E. Wieschaus, 2004a A nuclear function for armadillo/beta-catenin. PLoS Biol. **2:** E95.

Tolwinski, N. S., and E. Wieschaus, 2004b Rethinking WNT signaling. Trends Genet. **20:** 177–181.

Tolwinski, N. S., M. Wehrli, A. Rives, N. Erdeniz, S. DiNardo *et al.*, 2003 Wg/Wnt signal can be transmitted through arrow/LRP5,6 and Axin independently of Zw3/Gsk3beta activity. Dev. Cell **4:** 407–418.

Wagner, E., and J. Lykke-Andersen, 2002 mRNA surveillance: the perfect persist. J. Cell Sci. **115:** 3033–3038.

Wieschaus, E., C. Nusslein-Volhard and G. Jurgens, 1984 Mutations affecting the pattern of the larval cuticle in Drosophila melanogaster. III. Zygotic loci on the X-chromosome and fourth chromosome. Roux's Arch. Dev. Biol. **193:** 296–307.

Wodarz, A., U. Hinz, M. Engelbert and E. Knust, 1995 Expression of crumbs confers apical character on plasma membrane domains of ectodermal epithelia of Drosophila. Cell **82:** 67–76.

Wodarz, A., A. Ramrath, A. Grimm and E. Knust, 2000 Drosophila atypical protein kinase C associates with Bazooka and controls polarity of epithelia and neuroblasts. J. Cell Biol. **150:** 1361–1374.

Woods, D. F., and P. J. Bryant, 1989 Molecular cloning of the lethal(1)discs large-1 oncogene of Drosophila. Dev. Biol. **134:** 222–235.

Yamanaka, H., and E. Nishida, 2007 Wnt11 stimulation induces polarized accumulation of Dishevelled at apical adherens junctions through Frizzled7. Genes Cells **12:** 961–967.

Communicating editor: T. C. Kaufman